Tetrahedron 67 (2011) 1580–1588

Contents lists available at ScienceDirect

Tetrahedron

journal homepage: www.elsevier.com/locate/tet

Domino Diels–Alder reactions of *N*-methoxyethyl-7-oxa-norbornadiene-2, 3-dicarboximide: an elusive, highly reactive dienophile

Davor Margetić [a,*], Douglas N. Butler [b], Ronald N. Warrener [b], Yasujiro Murata [c]

[a] *Laboratory for Physical-Organic Chemistry, Division of Organic Chemistry and Biochemistry, Ruđer Bošković Institute, 10001 Zagreb, Croatia*
[b] *Centre for Molecular Architecture, Central Queensland University, Rockhampton, Queensland 4702, Australia*
[c] *Institute for Chemical Research, Kyoto University, Uji, Kyoto 611-0011, Japan*

ARTICLE INFO

Article history:
Received 6 October 2010
Received in revised form 23 November 2010
Accepted 13 December 2010
Available online 17 December 2010

Keywords:
Diels–Alder reaction
Furan
Flash vacuum pyrolysis
DFT calculations
Transition states

ABSTRACT

Flash vacuum pyrolysis (FVP) has been used to generate the novel 7-oxa-norbornadiene-2,3-dicarboxylic imide that in situ gave an unprecedented cycloaddition reaction cascade with the imidofuran, a side-product of FVP. Stereoselectivity of cycloadditions was studied with the aid of density functional calculations, which fully support observed *exo*/*endo*-selectivity.

1. Introduction

Norbornadiene and 7-hetero-norbornadiene-2,5-carboxylic anhydrides and imides are interesting for both synthetic and theoretical reasons. For instance, a computational study of these dienes[1] showed that both **1** and **2** have significantly pyramidalised substituted double bond (by 6.2° and 4.8°, respectively, using a DFT B3LYP/6-31G* calculations). These molecules are also highly reactive dienophiles, useful in the synthesis of sesquinorbornadienes.

We have previously used flash vacuum pyrolysis (FVP)[2] on anhydride **3**[3] to generate corresponding 7-oxanorbornadiene anhydride **2** (Scheme 1), but that FVP failed to produce its 7-aza and 7-thia counterparts.[4] Here we report the results of FVP experiments on corresponding imides **4a**–**d**.

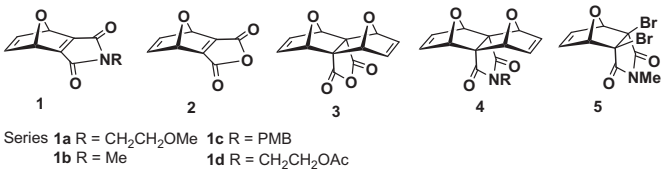

Scheme 1.

2. Results and discussion

Previously we have used a Zn/Ag debromination of imide **5** to prepare 7-oxanorbornadiene imide **1b**, which was trapped in situ with various cyclic dienes.[5] These conditions were too harsh to isolate and spectroscopically detect **1b**. An FVP route seemed to be more promising for the isolation and spectroscopic characterization of its counterpart **1a**. We also expected that adducts of imide **1a** would be more stable and have better chromatographic properties than those of anhydride **2** (due to anhydride susceptibility to hydrolysis) and so embarked on its synthesis.

2.1. FVP of 4a

In a series of experiments, it was found that FVP of imide **4a** at 375 °C (0.005 mbar) produced a mixture of products, while further increases of temperature to 390, 400, 420, 430, 445, and 480 °C gave increasingly more of the over-cracked product 2-methoxyethyl-1*H*,3*H*-pyrrolo[3,4-*c*]furan-1,3-dione **6a** (Scheme 2), with its distinctive aromatic singlet at δ 7.76. This was the most volatile product depositing furthest away from the pyrolysis oven, resulting in the total thermal destruction of starting material.[6] At 445 °C a yield of 54% of furan **6a** was obtained. Even at the lowest temperatures necessary to accomplish furan elimination, imide **6a** was detected, along with the substrate **4a**. The results suggest that retro Diels–Alder acetylene elimination in the imide case was easier than

* Corresponding author. Tel.: +385 1 456 1008; fax: +385 1 468 0195; e-mail address: margetid@irb.hr (D. Margetić).

0040-4020/$ – see front matter © 2010 Elsevier Ltd. All rights reserved.
doi:10.1016/j.tet.2010.12.032

from anhydride **3** to obtain **7**. However, we could not spectroscopically detect the desired imide **1a**.

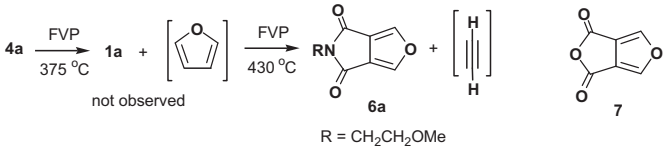

Scheme 2. End-products of FVP of **4a**.

All attempts to isolate the intermediate product **1a** were unfruitful so we have treated the FVP products with anthracene ($CHCl_3$, 60 °C 1 h) and were thus able to isolate four cycloadducts **9**–**12** by chromatographic separation (in 11, 13, 4, and 9% yields, respectively, Scheme 3). They originate from the domino Diels–Alder reaction[7] of *N*-methoxyethyl-7-oxanorbornadiene-2,3-dicarboximide **1a**, furan **6a**, and anthracene. Variation of FVP temperature causes a change in product composition (Table 1). When anthracene was added to the FVP tube prior a pyrolysis (excess), 1:1 cycloadduct **9** was formed exclusively (41% yield), while **6a** remained unreacted. This result suggests higher reactivity of anthracene than **6a**, probably due to the formation of less stable intermediate alkene adduct in the case of **6a**.

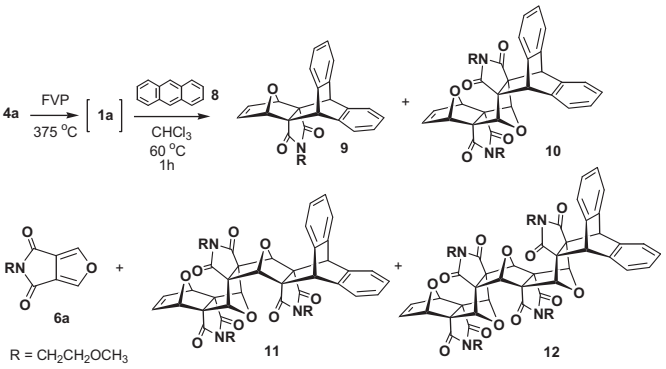

Scheme 3. FVP of **4a**.

Table 1
Ratios of cycloadducts, anthracene added after FVP[a]

T/°C	4a	6a	9	10	11	12
375	5	0.5	0.1	1	0.1	Trace
390	4	2	0.8	1	0.5	Trace
390[b]	10	1	1	—	—	—
400	1.5	1.5	1.1	1	1	0.1
420	0.4	1.5	0.7	1	1	0.1
430	0.1	1.1	0.1	0.2	—	—
445	0.4	1.5	0.7	1	1	0.1
480	0.1	2.01	0.5	0.2	—	—

[a] Obtained by ^{1}H NMR analysis.
[b] Anthracene added in FVP tube before pyrolysis.

Products **9**–**12** show increased spectral complexity, as illustrated in Fig. 1. For instance, the ^{1}H NMR of **12** contained of series of proton resonances, the most distinctive being vinylic δ 6.34, bridgehead (five lines) δ 4.65, 4.69, 4.79, 4.86, 4.92, and methoxy (four lines) δ 3.09, 3.23 (two signals overlapped), 3.23, which is completely consistent with the assigned structure, and further supported by the 32-line ^{13}C NMR, and high-resolution mass spectrometry (m/z=984.3065, calcd 984.3065). Spectral data for all adducts supports a stereoselective Diels–Alder reaction, giving only *exo*,*endo*-adducts. *exo*-Structure of cycloadduct **9** was elucidated from its spectral data, C_s symmetry and compared with the independently prepared *N*-methyl derivative **9b** (by debromination of **5** and trapping with anthracene). Proton NMR

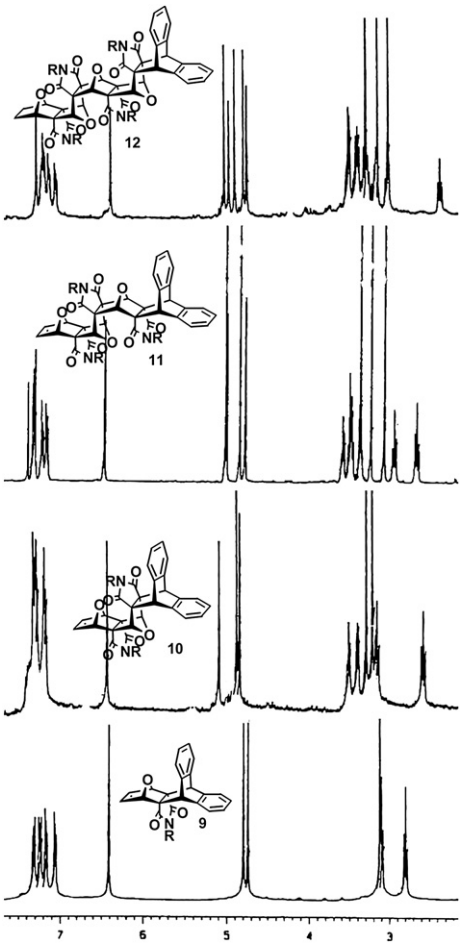

Fig. 1. Mid-portion of ^{1}H NMR spectra of adducts **9**–**12**.

spectra showed that aromatic shielding caused the chemical shift of the CH_2 protons in product **9** from 3.36 ppm in **4a** to 2.81 ppm. In products **10**–**12**, the shielding is only found for the methylene group, which is adjacent to the anthracene unit. The CH_2 proton signals are shifted to even higher fields (2.52, 2.52, and 2.34 ppm, respectively), where the methylene protons in adduct **12** experience the largest shielding. The methoxy groups are apparently not so shielded, but still follow the same descending order (**9**–**12**: 3.13, 2.99, and 2.96 ppm, in **4a** 3.29 ppm). On the other hand, the olefinic protons in **9** were shielded to a lesser extent (6.58 ppm in **4a** vs 6.41 ppm in **9**). However, these shieldings alone were not sufficient to assign the exact stereochemistry of products. Hence, the combined results of 2D NMR (COSY and NOESY experiments) and molecular modeling were used for structural elucidation of **10**–**12**.

Molecular modeling (BLYP/6-31G*) of adducts with the *exo*,*exo*-stereochemistry indicates that protons of the two methylene groups positioned on neighboring imide nitrogens are separated by 2.61 Å, while the proximal bridgehead protons are separated by 2.52 Å. For this structure, positive NOE correlations were expected. In the case of *exo*,*endo*-stereochemistry bridgehead protons are separated by 3.41 Å, for which weak NOE correlation is assumed. Therefore, the lack of NOE correlations between the ethylene triplets on neighboring imide nitrogens, and the lack of NOE correlations among bridgehead singlets were suggestive of an *exo*,*endo*-stereochemistry.

Experimental data suggest that the initially formed imide **1a** and the imidofuran **6a** reacted further in a domino manner, either in the pyrolysis furnace, or out in the tube, since they have similar

volatilities and deposit together on the cooler parts of the pyrolysis tube. Here, imidofuran **6a** acts both as a diene and a masked dienophile, whose dienophilic character is developed after initial Diels–Alder cycloaddition. This domino reaction gave at the first instance, the 1:1 adduct **13**, which was also reactive dienophile, producing the domino 2:1 adduct **14** and the 3:1 adduct **15** (Scheme 4). It is possible that some higher domino cycloadducts were formed and that these have not been detected. When a chromatographic workup was applied to the mixture of products **13**–**15**, we have been able to spectroscopically detect adducts **13** and **14** in partially purified form, as well as hydrolysis product **13b**. The key spectroscopic evidence for intermediate cycloadduct **13** are two methyl and two bridgehead proton resonances and the molecular ion (^{1}H NMR: δ NMe 3.31, 3.32, δ bridgehead 4.80, 5.57, HRMS-ESI: m/z=416.1223), while for **14** three methyl and three bridgehead resonances were found (^{1}H NMR: δ NMe 3.18, 3.19, 3.29, δ bridgehead 4.70, 5.03, 5.59, HRMS-ESI: m/z=587.1754).

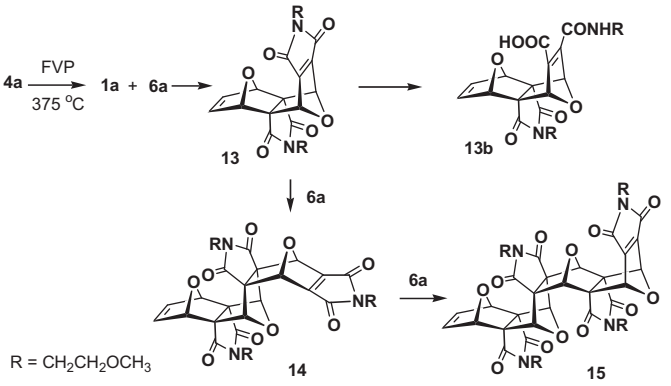

Scheme 4. Intermediate products in FVP of **4a**.

2.2. FVP of 4b–d

FVP of the corresponding *N*-methyl imide **4b** (at 395 °C, 0.001 mbar) gave a similar complex mixture to **4a** and no attempts was made to separate the reaction mixture. When the temperature was raised to 440 °C furan **6b** was formed as a major product. Again, no conclusive spectroscopic evidence of formation of imide **1b** was obtained.

Inconsistent results were obtained in the case of *p*-methoxybenzyl (PMB) substituted imide **4c** (Scheme 5). Thus, FVP of **4c** at 360 °C yielded a complex mixture of products, which was separated by chromatography. Most notable differences in comparison with products obtained by FVP of **4a** are the lack of higher 3:1 and 4:1 adducts. In addition, imidofuran **6c** was not detected, presumably due to its instability in the reaction conditions. Experimental support for this explanation is given by the exclusive formation of 1:1 and 2:1 adducts **17** (18% yield) and **18** (10%), and the presence of larger proportion of polymeric material as compared to FVP of **4a**. The ^{1}H NMR spectrum of **17** consists eight singlets (δ 3.77, 3.79, 3.99, 4.29, 4.66, 4.76, 4.91, and 5.87) and eight aromatic multiplets (δ 6.60, 6.70, 6.74, 6.77, 6.98, 7.11, 7.12, and 7.21), while the ^{13}C NMR exhibited 22 resonances. Surprisingly, instead of substituted 1:1 cycloadduct **16**, deprotected 1:1 adduct **18** was isolated and fully characterized by means of 1D NMR spectroscopy and X-ray structural analysis (Scheme 4). The ^{1}H NMR spectrum of **18** shows three singlets and four aromatic multiplets, while ^{13}C NMR contains eleven carbon resonances, m/z=341.1056 calcd 341.1052. The most characteristic feature of **18** was the proton resonance of imide group positioned at 6.69 ppm. Several PMB group deprotection methods were published,[8] for the specific dioxanorbornene **4c**

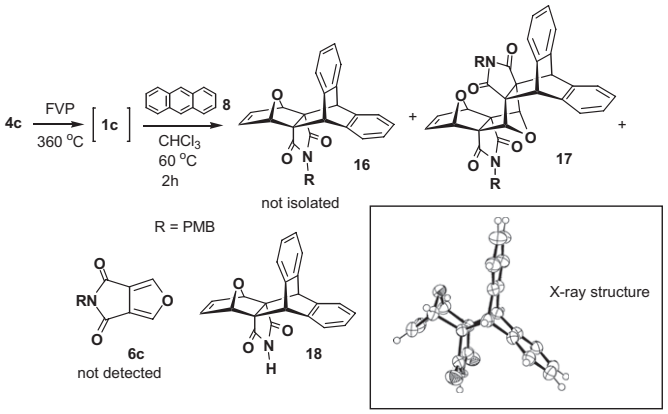

Scheme 5. FVP of **4c**.

substrate: cerium(IV) ammonium nitrate was used,[9] while FVP conditions used in our work are better replicated by reflux heating in TFA, or MW irradiation in TFA/DCM at 120 °C.[8]

Studies on related imides showed that FVP of acetate **4d** required slightly higher temperature than **4a** (420 °C). Imidofuran **6d** is the dominant product in the mixture, as indicated by its distinctive aromatic singlet at δ 7.80. The presence of **6d** is even more pronounced in the FVP experiment carried out at 460 °C (Scheme 6). Even at this temperature, significant amount of uncracked imide **4d** is present. The detailed ^{1}H NMR analysis of the reaction mixture revealed that alongside **6d** cycloadducts **19** and **20** were formed in approx. 1:1.5 ratio. For the formation of **19** indicative is the presence of two bridgehead proton resonances (singlets, δ 4.73, 4.96), while in the case of **20** one may found three (δ 4.65, 4.91, 4.94). Aromatic ring shielding caused the ^{1}H NMR chemical shift of the ethylene triplets in product **30** to 2.82 and 3.32 ppm (**4d**: 3.47 and 4.03 ppm), while in **20** these resonances are found at 3.13 and 3.24 ppm. Methyl proton resonances in **19** and **20** were also shifted to higher field, 1.89 and 1.77 ppm, respectively (starting from 2.00 ppm in **4d**).

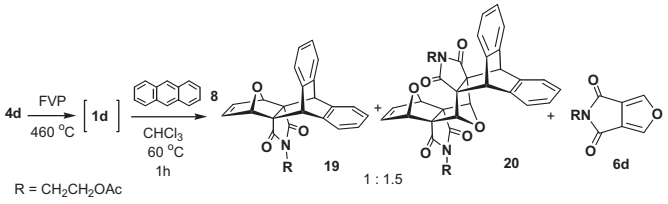

Scheme 6. FVP of **4d**.

Further synthetic studies showed that 7-oxanorborneno imide **21**[10], a partially saturated counterpart of 7-oxanorbornadieno imide **4b** showed similar chemical behavior in the pyrolysis furnace (Scheme 7). Thus, FVP of **21** at 380 °C yielded a mixture of products, in which furanoimide **6b** dominates. Reduction of FVP temperature to 340 °C gave a mixture of **21**, **22**, **6b**, and **25** in a 0.8:3.4:0.1:0.2 ratio. While the existence of the intermediate product **1a** could not be proven by means of ^{1}H NMR spectroscopy, it was possible to detect its saturated counterpart **22** in the crude pyrolysate (δ NMe 2.96, δ bridgehead 5.36, m/z=179.0580). Its formation was previously indirectly proven by hydrogenation reactions of imide **5**.[10] In addition, the intermediate cycloadduct **25** was spectroscopically observed (δ NMe 3.00, 3.02, δ bridgehead 4.44, 5.59) and confirmed by mass spectrometry (m/z=330.0850). These reactive intermediates could not be isolated, but were converted to the corresponding anthracene cycloadducts **23** and **24** by heating at 70 °C for 1 h in chloroform solution. Products **23** and **24** were isolated in 35% and 5% yield, respectively.

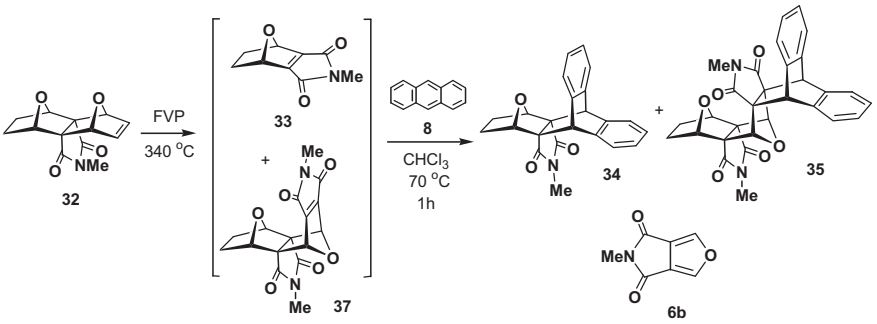

Scheme 7. FVP of **21**.

2.3. Microwave reactions

It is known that rates of Diels–Alder[11] and retro Diels–Alder reactions are accelerated under microwave conditions.[12] Since recent literature reports showed that FVP conditions could be successfully replaced by MW conditions,[13] we anticipated that both reactions (conducted in single reaction pot) will benefit from rate enhancement by microwave irradiation. Thus, the 7-oxanorborneno maleimide **4a** was subjected to microwave heating in order to compare microwave and FVP conditions. Samples of **4a** were heated in a closed-vial single mode MW reactor for 5 min at temperatures varying from 200 to 250 °C (power 250 W). At 200 °C, maleimide **4a** was recovered unchanged, while at temperatures above 230 °C, ^{1}H NMR gave no spectral support for the production of expected cycloadducts in the crude pyrolysate, whereas **4a** starts to decompose forming complex mixture consisting mainly of polymers. Similar results were obtained with maleimide **4c** (MW at 200–220 °C, 5 min).

2.4. Quantum-chemical calculations

The origins of the experimentally observed stereoselectivities obtained in domino Diels–Alder reactions of **1a** and furan **6** and additional support for structural assignments were sought computationally. For this purpose, transition state calculations, using density functional theory (DFT) were employed. A standard B3LYP/6-31G* method was used. In addition, two recently developed DFT functionals were employed (BMK[14] and M052X[15]), which are specifically designed for obtaining better reaction energetics. Since flexibility of methoxyethyl substituents in **1a** and **6** significantly increases computational time, $CH_2CH_2OCH_3$ groups were replaced by an H atom. This simplified reaction system is still a valid model, since all important structural and electronic features of studied system remained. There are four possible modes of diene approach to the π-bond of norbornadiene of type **1a**: two of these are from the top (*exo*-) face (*exo*,*exo*- and *exo*,*endo*-**TS1** and **TS2**) (defined in the respect to the norbornene moiety), and two approaches are from the bottom (*endo*-) face (*endo*,*endo*- and *endo*,*exo*-**TS3** and **TS4**). Modes of approach of diene **6** to 1:1 and 2:1 adducts were named accordingly. A summary of the computational results is given in Fig. 2.

The calculated transition state geometries represent a concerted, synchronous cycloaddition mechanism, as illustrated in Fig. 3 for **TS1** and **TS2**. The most interesting aspect of the calculated geometries is the length of the newly formed bonds between the dipole and dipolarophile. Survey of the data reveals that the newly forming C···C bonds are separated by 2.175–2.325 Å, which are slightly longer than the bond lengths calculated for a series of hydrocarbon pericyclic reactions.[30] These TS structures possess five-membered furan moiety where the oxygen atom is tilted away from planarity by α=25.8 and 15.0°, respectively.

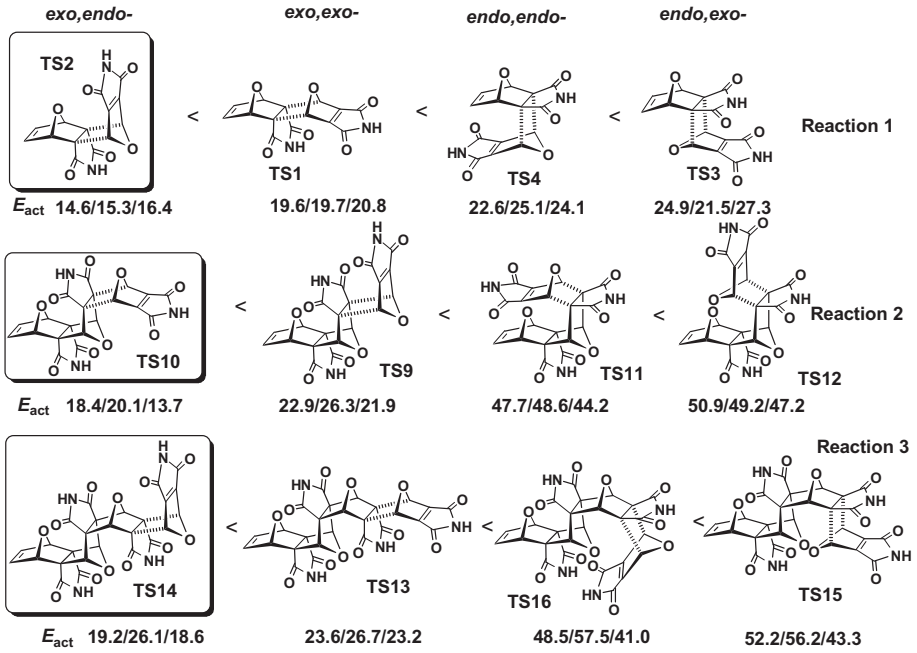

Fig. 2. B3LYP/6-31G*, BMK/6-31G*, and M052X/6-31G* activation energies (kJ mol^{-1}).

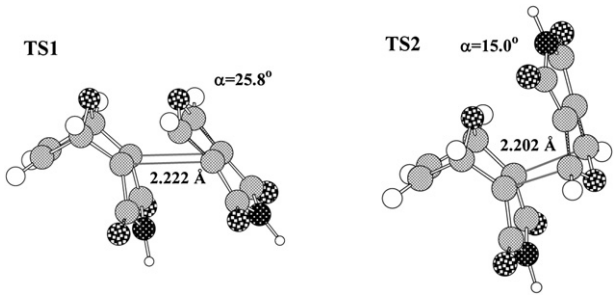

Fig. 3. B3LYP/6-31G* optimized structures of **TS1** and **TS2**.

The hybrid density functionals B3LYP, BMK, and M052X showed very good qualitative agreement amongst themselves. Therefore, we may conclude with a confidence that **TS2** has the smallest E_a, while the relative activation energies increase in the following order: E_a(**TS2**)<E_a(**TS1**)<E_a(**TS4**)<E_a(**TS3**); E_a(**TS10**)<E_a(**TS9**)<E_a(**TS11**)<E_a(**TS12**); and E_a(**TS14**)<E_a(**TS13**)<E_a(**TS16**)<E_a(**TS15**). The DFT[16] calculations clearly indicate that the approach of diene (imidofuran) **6** from the *exo*-face of the dienophile is energetically preferred over *endo*-approach (Fig. 2). Regardless of the functional used, preference for *exo*-addition were always obtained. Furthermore, energy differences between *exo*,*exo*- and *exo*,*endo*-TSs are larger than 4 kcal mol^{-1}, which indicates that reactants could achieve stereoselective cycloadditions.[17] The addition of the second and third molecule of **6** also favors an *exo*,*endo*-approach (in **TS10** and **TS14**) by 4.5 kcal mol^{-1}. This conclusion is in full accordance with our experimental data. The comparison of B3LYP with new BMK and M052X DFT methods, showed that both methods perform well for this particular reaction, giving relative E_as, which are very close to those estimated by B3LYP functional.

An interesting observation is the dramatic increase in activation energy for *endo*-addition going from the first reaction (**TS3** and **TS4**) to reactions 2 and 3 (**TS11**, **TS12**, **TS15**, and **TS16**). This difference could be rationalized by a significant increase in steric interactions of the incoming diene with the 7-oxanorbornane bridge, which does not exist in **TS3** and **TS4**. These predictions are in good accordance with previously published experimental and theoretical results on norbornene π-facial selectivity.[18–22] Plausible explanation for preferred *exo*-addition to the π-bond of norbornadiene of type **1a** may be offered in terms of the non-equivalent orbital extension and double bond pyramidalization. Pyramidalization angles of 6.2, 12.4, and 11.6° were calculated for norborene reactants **13** (R=H), **14** (R=H), and **15** (R=H), at the B3LYP/6-31G* level, respectively. Reactants **14** (R=H) and **15** (R=H) are norbornenes, which are always more pyramidalized than corresponding norbornadienes, due to electronic interactions.[23] It could be seen that relative activation energies are not correlated with the extent of pyramidalization, indicating that other factors play an important role in determining their reactivity. The other factor governing the preference to *exo*-addition to the π-bond of norbornadiene of type **1a** was identified as non-equivalent orbital extension.

Fig. 4 depicts the LUMO of reactant **13** (R=H), plotted on electron density isosurface. The inspection of isosurfaces reveals that there is orbital non-equivalency between the *exo*- and *endo*-π-faces. There is a larger electron density located on the *exo*-face,[24] which in the combination with the steric hindrance imposed at the *endo*-face contributes to the *exo*-face preference.[25]

Repulsive steric interactions are nicely visualized when *N*-methoxyethyl substituents were added, such as in the product **12** (Fig. 5c). Furthermore, Fig. 5 depicts electrostatic potential surfaces for **TS13** and **TS14**. Here repulsive *O*—*O* lone electron pair interactions in the case of the *exo*,*exo*-approach in **TS13** are clearly visible, indicating that *exo*,*endo*-approach (**TS14**) is preferred.

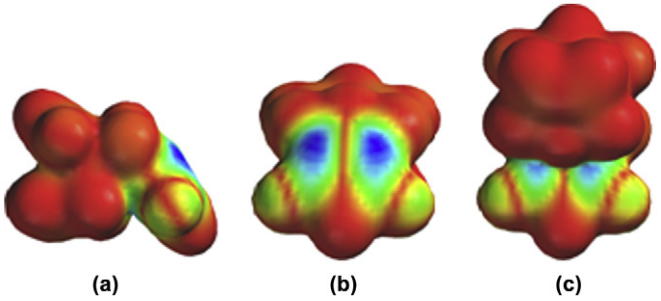

Fig. 4. LUMO of **13**(R=H) plotted on electron density isosurface (isovalue=0.002 electrons/au^3): (a) side-view, (b) *exo*-face, (b) *endo*-face, (c) *exo*-face.

3. Conclusion

Flash vacuum pyrolysis (FVP) has been used as a powerful tool to generate the novel 7-oxa-norbornadiene-2,3-dicarboxylic imide that in situ gave a domino Diels—Alder cycloaddition reaction cascade with over-cracked furanoimide. The furanoimide product behaves in an unprecedented manner, firstly as 1,3-diene, and after cycloaddition, takes place in subsequent Diels—Alder reaction as a highly potent dienophile. Exclusive formation of *exo*,*endo*-adducts in these cycloadditions was studied by the aid of density functional calculations and rationalized by the *exo*-pyramidalization of norbornene π-bond, steric and oxygen lone pair repulsions. The 1*H*,3*H*-pyrrolo[3,4-*c*]furan-1,3-diones **6a** and **7** are interesting novel dienes/masked dienophiles, which, upon Diels—Alder reaction deliver highly activated dienophilic double bonds, and the synthetic uses of these observations are currently being investigated in our laboratories.

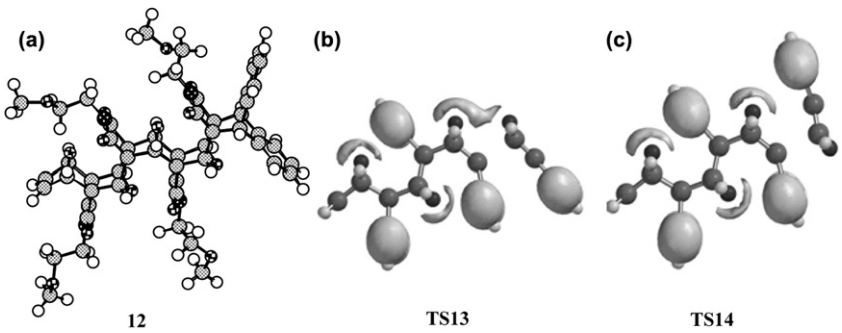

Fig. 5. (a) B3LYP/6-31G* optimized structure of product **12** and electrostatic potential surfaces for (b) **TS13**, (c) **TS14** (isovalue=−20 au).[26,27]

4. Experimental part

4.1. General

The NMR spectra were recorded in $CDCl_3$ solutions containing tetramethylsilane as internal standard on a Bruker AMX-300 or a Bruker Avance DPX-400 NMR spectrometer fitted with a gradient quattro nucleus probe. Melting points were determined using a Gallenkamp digital melting point apparatus and are uncorrected. The high-resolution mass spectra were recorded on a Micromass Platform II single quadrupole AutoSpec instrument (ESMS, electrospray mass spectrometry in CH_2Cl_2). Radial chromatography was carried out with a chromatotron, Model No. 79245 T, using 1 mm plates with silica gel 60 F_{254} as the stationary phase.

Flash-vacuum experiments were conducted under vacuum (0.001 mbar) in a 600×10 mm Pyrex tube heated by a horizontally mounted 'Thermolyne' model 21100 tube furnace. Products were collected at the end of furnace on cooler part of the tube. Volatile products (furan and acetylene) were condensed in liquid nitrogen trap. All new compounds were isolated by radial chromatography and gave satisfactory spectroscopic and analytical data (accurate mass).

Microwave assisted reactions were conducted in CEM Discover®LabmateTH/ExplorerPLS® single mode microwave reactor using closed reaction vessel technique (power=125 W).

N-2-Methoxyethyl carboximide precursor **4a** was prepared by previously published procedure,[28] by reaction of anhydride **3** with methoxyethyl amine, followed by cyclisation with acetic anhydride.

*4.1.1. (2α,5α,7α,10α)-12-Methoxyethyl-12-aza-14,15-dioxapenta cyclo[4.4.3.1^{2,5}.1^{7,10}.0^{2,7}] pentadeca-3,8-diene-11,13-dione (**4b**)*[11]. An aq ueous solution of methylamine (25–30%, 3 mL) was added dropwise to an ice-cooled solution of anhydride **3** (645 mg, 2.783 mmol) in ethanol (5 mL). The solution was allowed to stir at room temperature for 2 h. The solvent was evaporated under reduced pressure (water bath temperature 20–30 °C) to give the intermediate amic acid as brown oil. Without further purification, this oil was treated with Ac_2O (2 mL), NaOAc (400 mg), and the mixture stirred at 50–60 °C for 1 h. The solvent was evaporated under high vacuum, residue dissolved in CH_2Cl_2, washed with water, dried over $MgSO_4$, and the solvent was evaporated off to produce solid material, which was recystallised from EtOAc to yield the *title compound* **4b** as colorless crystals (300 mg, 44%, mp 241–244 °C).

δ_H (400 MHz, $CDCl_3$) 6.62 (2H, t, *J*=0.9 Hz), 5.26 (2H, t, *J*=0.9 Hz), 2.72 (3H, s); δ_C (100 MHz, $CDCl_3$) 174.4, 139.2, 81.4, 69.6, 24.6; ν_{max} (KBr) 3129, 1726, 1226 cm^{-1}; HRMS (ESI): M$^+$, found 245.0692, $C_{13}H_{11}NO_4$ requires 245.0688.

*4.1.2. (2α,5α,7α,10α)-12-(p-Methoxybenzyl)-12-aza-14,15-dioxa pentacyclo[4.4.3.1^{2,5}.1^{7,10}.0^{2,7}] pentadeca-3,8-diene-11,13-dione (**4c**)*[9]. *p*-Methoxybenzylamine (411 mg, 4 mmol) was added dropwise to an ice-cooled solution of anhydride **3** (262 mg, 1.129 mmol) and Et_3N (1 mL) in CH_2Cl_2 (5 mL). The solution was allowed to stir at room temperature for 24 h. The solvent was evaporated under reduced pressure (water bath temperature 20–30 °C) to give the intermediate amic acid as brown oil. Without further purification, this oil was treated with Ac_2O (2 mL) and Et_3N (1 mL), and the mixture stirred at 50–60 °C overnight. The solvent was evaporated under high vacuum, residue dissolved in CH_2Cl_2, washed with water, dried over $MgSO_4$, and the solvent was evaporated to produce solid material, which was recystallised from EtOAc to yield colorless crystals of the *title compound* **4c** (142 mg, 36%).

δ_H (400 MHz, $CDCl_3$) 7.17 (2H, d, *J*=8.6 Hz), 6.80 (2H, d, *J*=8.6 Hz), 6.39 (4H, s), 5.21 (4H, s), 4.29 (2H, s), 3.79 (3H, s).

*4.1.3. (2α,5α,7α,10α)-12-(Acetoxyethyl)-12-aza-14,15-dioxapenta cyclo [4.4.3.1^{2,5}.1^{7,10}.0^{2,7}] pentadeca-3,8-diene-11,13-dione (**4d**).* Ethanolamine (7 mL) was added dropwise to an ice-cooled solution of anhydride **3** (3.00 g, 12.931 mmol) in $CHCl_3$ (60 mL). The solution was allowed to stir at room temperature for 12 h. To this mixture Ac_2O (12 mL) was added and stirred below 25 °C for 12 h. The solution containing solid was cooled in an ice bath, precipitate collected by filtration and washed with cooled chloroform. Amic acid (4.0 g) was dissolved in Ac_2O (25 mL) and Et_3N (4 mL), and the mixture stirred at 50–60 °C for 3 days. Reaction mixture was cooled to room temperature, precipitate collected by filtration, and washed with water to obtain **4d** as colorless crystals (2.8 g). Mother liquor was evaporated off under high vacuum, and solid material was washed with water to obtain additional amount of the *title compound* **4c** (850 mg, total yield 64.6%, mp 186–188 °C).

δ_H (400 MHz, $CDCl_3$) 6.59 (4H, s), 5.26 (4H, s), 4.04 (2H, t, *J*=5.12 Hz), 3.48 (2H, t, *J*=5.12 Hz), 2.02 (3H, s), δ_C (100 MHz, $CDCl_3$) 174.4, 170.6, 139.4, 81.6, 69.7, 60.9, 37.7, 21.1; ν_{max} (KBr) 3144, 1693, 1678, 1393, 1206 cm^{-1}; HRMS (ESI): M$^+$, found 347.1372, $C_{18}H_{21}NO_6$ requires 347.13689.

FVP of **4a**. In a typical run, FVP of **4a** (30 mg, 0.104 mmol) at 420 °C produced a mixture, which was dissolved in chloroform (1–2 mL) and treated with anthracene (100 mg, 0.561 mmol) for 2 h at 60 °C. Reaction mixture was subjected to radial chromatography (petroleum ether–ethyl acetate 10:1, then the solvent polarity was gradually increased to 1:1) to obtain products, in order of elution: anthracene, **6a**, **4a**, **9**, **10**, **11**, and **12**.

*4.1.4. 1-Methoxyethyl-1-aza-5-oxabicyclo[3.3.0^{3,7}]octa-3,6-diene-2,8-dione (**6a**).* Compound **6a** (18 mg, 40%, mp 104–106 °C); δ_H (400 MHz, $CDCl_3$) 7.76 (2H, s), 3.82 (2H, t, *J*=5.6 Hz), 3.59 (2H, t, *J*=5.6 Hz), 3.34 (3H, s); δ_C (100 MHz, $CDCl_3$) 69.2, 161.6, 138.7, 122.4, 58.6, 37.8; ν_{max} (KBr) 3047, 1788, 1599, 1389, 1219 cm^{-1}; HRMS (ESI): M$^+$, found 195.0529, $C_9H_9NO_4$ found 195.0531.

*4.1.5. (2α,9α,11α,14α)-16-Methoxyethyl-16-aza-18-oxahepta cyclo[8.4.3.4^{2,9}.1^{11,14}.0^{1,10}.0^{2,9}.0^{3,8}]tetracosa-3,5,7,12,19, 21,23-heptaene-15,17-dione (**9**).* Compound **9** (9 mg, 11%, mp 108–111 °C); δ_H (400 MHz, $CDCl_3$) 7.32 (2H, dd, *J*=3.3 , 5.5 Hz), 7.24 (2H, dd, *J*=3.3 , 5.5 Hz), 7.18 (2H, dd, *J*=3.1 , 5.5 Hz), 7.07 (2H, dd, *J*=3.1 , 5.5 Hz), 6.41 (2H, s), 4.81 (2H, s), 4.75 (2H, s), 3.11 (2H, t, *J*=6.2 Hz), 3.13 (3H, s), 2.81 (2H, t, *J*=6.2 Hz); δ_C (100 MHz, $CDCl_3$) 176.4, 141.5, 140.0, 137.8, 126.9, 126.7, 125.0, 124.4, 81.7, 68.0, 65.2, 58.4, 48.1, 37.2; ν_{max} (KBr) 3019, 1766, 1426, 778 cm^{-1}; HRMS (ESI): M$^+$, found 397.1318, $C_{25}H_{21}NO_4$ requires 397.1314.

*4.1.6. (2β,4α,11α,13β,15α,18α)-20,29-Di(methoxyethyl)-20,29-diaza-31,32-dioxaoctacyclo [12.4.3.6.^{4,11}.3^{3,12}.1^{2,13}.1^{15,18}.0^{1,14}.0^{3,12}.0^{5,10}.0^{22,27}] dotriaconta-5,7,9,16,22,24,26-heptaene-19,21,28,30-tetraone (**10**).* Compound **10** (8 mg, 13%, mp 233–234 °C); δ_H (400 MHz, $CDCl_3$) 7.22–7.31 (4H, m), 7.11–7.16 (4H, m), 6.34 (2H, s), 4.95 (2H, s), 4.74 (2H, s), 4.70 (2H, s), 3.41 (2H, t, *J*=5.8 Hz), 3.29 (2H, t, *J*=5.8 Hz), 3.21 (3H, s), 3.12 (3H, s), 3.07 (2H, t, *J*=6.3 Hz), 2.52 (2H, t, *J*=6.3 Hz); δ_C (100 MHz, $CDCl_3$) 175.9, 175.7, 140.9, 140.4, 138.2, 127.8, 127.5, 125.8, 125.4, 84.0, 78.4, 68.7, 68.4, 58.8, 49.04, 40.0, 39.2, 37.9, 37.8; ν_{max} (KBr) 2989, 1769, 1753, 1346, 1293 cm^{-1}; HRMS (ESI): M$^+$, found 594.1994, $C_{52}H_{48}N_4O_6$ requires 594.2002.

*4.1.7. (2α,4α,11α,13α,15β,17α,20α,22β)-24,33,36-Tri(methoxy ethyl)-24,33,36-triaza-38,39,40-trioxadodecacyclo[12.8.3.6.^{4,11}.3^{3,12}.3^{16,21}.1^{2,13}.1^{15,22}.1^{17,20}.0^{1,14}.0^{3,12}.0^{5,10}.0^{16,21}.0^{26,31}]tetratriaconta-5,7,9,18,26,28,30-heptaene-23,25,32,34,35,37-hexaone (**11**).* Compound **11** (6 mg, 4%, mp 240–242 °C); δ_H (400 MHz, $CDCl_3$) 7.19 (4H, dd, *J*=3.3 , 5.3 Hz), 7.09 (2H, dd, *J*=3.1 , 5.3 Hz), 7.04 (2H, dd, *J*=3.1 , 5.3 Hz), 6.34 (2H, s), 4.65 (2H, s), 3.45 (2H, t, *J*=5.8 Hz), 3.36 (2H, t, *J*=5.8 Hz), 3.35 (2H, t, *J*=6.7 Hz), 3.23 (3H, s), 3.21 (2H, t, *J*=6.7 Hz), 3.09 (3H, s), 2.99 (3H, s), 2.79 (2H, t, *J*=6.9 Hz),

2.52 (2H, t, J=6.9 Hz); δ_C (100 MHz, $CDCl_3$) 175.7, 174.5, 174.4, 140.2, 139.8, 138.2, 127.4, 127.0, 125.5, 124.5, 87.1, 79.6, 78.1, 71.5, 69.7, 69.0, 68.6, 68.1, 64.8, 59.4, 58.7, 58.5, 51.9, 39.5, 38.6, 35.8; ν_{max} (KBr) 3045, 1773, 1748, 1732, 1597, 1593, 1592, 1406 cm^{-1}; HRMS (ESI): M^+, found 789.2133, $C_{43}H_{39}N_3O_{12}$ requires 789.2533.

*4.1.8. (2α,4β,6α,9α,11β,13α,15β,17α,24α,26β)-28,37,40,43-Tetra (methoxyethyl)-28,37,40,43-tetraaza-45,46,47,48-tetraoxapenta decacyclo [12.12.3.6.^{17,24}.3^{3,12}.3^{5,10}.3^{16,25}.1^{2,13}.1^{4,11}.1^{6,9}.1^{15,26}.0^{1,14}.0^{3,12}.0^{5,10}.0^{16,25}.0^{18,23}.0^{30,35}]octatetraconta-7,18,20,22,30,32,34-heptaene-27,29,36,38,39,41,42,44-octaone (**12**).* Compound **12** (3 mg, 9%, mp 268–270 °C); δ_H (400 MHz, $CDCl_3$) 7.19 (2H, dd, J=3.3 , 5.1 Hz), 7.15 (2H, dd, J=3.3 , 5.3 Hz), 7.17 (2H, dd, J=3.3 , 5.1 Hz), 7.03 (2H, dd, J=3.3 , 5.3 Hz), 6.34 (2H, s), 4.92 (2H, s), 4.86 (2H, s), 4.79 (2H, s), 4.69 (2H, s), 4.65 (2H, s), 3.42–3.44 (4H, m), 3.30–3.38 (4H, m), 3.23 (6H, s), 3.20 (2H, t, J=6.8 Hz), 3.11 (2H, t, J=6.8 Hz), 3.09 (3H, s), 2.97 (2H, t, J=7.1 Hz), 2.96 (3H, s), 2.34 (2H, t, J=7.1 Hz); δ_C (100 MHz, $CDCl_3$) 175.8, 174.4, 174.3, 173.7, 140.8, 140.3, 138.2, 127.8, 127.1, 125.6, 124.5, 87.7, 82.6, 79.6, 78.1, 71.4, 70.1, 68.9, 68.6, 68.5, 68.4, 64.7, 58.9, 58.7, 51.8, 39.7, 39.0, 38.8, 37.5, 33.2, 30.9, 29.8; ν_{max} (KBr) 3040, 1786, 1766, 1751, 1720, 1578, 1443, 1374 cm^{-1}; HRMS (ESI): M^+, found 984.3065, $C_{52}H_{48}N_4O_{16}$ requires 984.3065.

FVP of **4a** (30 mg, 0.104 mmol) at 445 °C produced a mixture, which was subjected to radial chromatography (petroleum ether–ethyl acetate 10:1) to obtain **6a** (11 mg, 54%).

FVP of mixture of **4a** (50 mg, 0.173 mmol) and anthracene (200 mg, excess) at 390 °C produced a mixture, which was subjected to radial chromatography (petroleum ether–ethyl acetate 10:1, then the solvent polarity was gradually increased to 1:1) to obtain products, in order of elution: anthracene, **6a** (11 mg, 33%) and **9** (28 mg, 41%).

FVP of **4a** (30 mg, 0.104 mmol) at 420 °C produced a mixture, which was subjected to radial chromatography (petroleum ether–ethyl acetate 10:1) to obtain in order of elution: **6a**, **4a**, and purified **13**, **14**, and **13b**.

*4.1.9. (2β,8β,10α,13α)-5,15-Di(methoxyethyl)-5,5-diaza-17,18-dioxahexacyclo[7.4.3.1^{2,8}.1^{10,13}.0^{1,9}.0^{3,7}]octadeca-3,11-diene-4,6,14,16-tetraone (**13**).* (Spectral data obtained from crude spectrum); δ_H (400 MHz, $CDCl_3$) 6.53 (2H, t, J=0.9 Hz), 5.57 (2H, s), 4.80 (2H, t, J=0.9 Hz), 3.70 (2H, t, J=5.5 Hz), 3.62 (2H, t, J=5.5 Hz), 3.49 (2H, t, J=5.5 Hz), 3.46 (2H, t, J=5.5 Hz), 3.32 (3H, s), 3.31 (3H, s); HRMS (ESI): M^+, found 416.1223, $C_{20}H_{20}N_2O_8$ requires 416.1219.

*4.1.10. 4-Carboxymethoxyethyl-(2β,8β,10α,13α)-12-methoxy ethyl-12-aza-14,15-dioxapentacyclo[4.4.3.1^{2,5}.1^{7,10}.0^{1,6}] pentadeca-3,8-diene-11,13-dione-3-carboxylic (**13b**).* (Spectral data obtained from crude spectrum); δ_H (400 MHz, $CDCl_3$) 6.45 (1H, dd, J=1.3 , 5.6 Hz), 6.44 (1H, dd, J=1.3 , 5.6 Hz), 5.49 (1H, d, J=2.4 Hz), 5.56 (1H, s), 5.10 (1H, s), 4.72 (1H, d, J=3.7 Hz), 3.42–3.73 (8H, m), 3.36 (3H, s), 3.32 (3H, s); HRMS (ESI): M^+, found 434.1321, $C_{20}H_{22}N_2O_9$ requires 434.1325.

*4.1.11. (2β,4α,7α,9β,11α,17α)-14,19,22-Tri(methoxyethyl)-14,19, 22-triaza-24,25,26-trioxaonacyclo[8.7.3.3.^{3,8}.1^{2,9}.1^{4,7}.1^{11,17}.0^{2,9} .0^{4,7}.0^{11,17}] hexacosa-5,12-diene-13,15,18,20,21,23-hexaone (**14**).* (Spectral data obtained from crude spectrum); δ_H (400 MHz, $CDCl_3$) 6.53 (2H, s), 5.59 (2H, s), 5.03 (H, s), 4.70 (2H, s), 3.35–3.85 (12H, s), 3.29 (3H, s), 3.19 (3H, s), 3.18 (3H, s); HRMS (ESI): M^+, found 587.1754, $C_{27}H_{29}N_3O_{12}$ requires 587.1751.

*4.1.12. (2α,9α,11α,14α)-16-Methyl-16-aza-18-oxaheptacyclo[8.4.3.4^{2,9}.1^{11,14}.0^{1,10}.0^{2,9}.0^{3,8}]tetracosa-3,5,7,12,19, 21,23-heptaene-15,17-dione (**9b**).* To a refluxing solution of dibromide **5** (100 mg, 0.297 mmol) and anthracene (200 mg, excess) in dry THF (10 mL) at reflux, freshly prepared Zn–Ag couple (200 mg) was added and refluxed for 1 h. Filtration and evaporation of solvent gave a brown colored oil, which was subjected to radial chromatography (petroleum ether–ethyl acetate 10:1, then solvent polarity was gradually increased to 1:1) to afford the *title compound* **9b** as a colorless solid (61 mg, 58%, mp 176–178 °C).

δ_H (400 MHz, $CDCl_3$) 7.33 (2H, dd, J=3.1 , 5.3 Hz), 7.25 (2H, dd, J=3.1 , 5.3 Hz), 7.18 (2H, dd, J=3.3 , 5.5 Hz), 7.05 (2H, dd, J=3.3 , 5.5 Hz), 6.43 (2H, s), 4.81 (2H, s), 4.75 (2H, s), 2.34 (3H, s); δ_C (100 MHz, $CDCl_3$) 176.6, 141.5, 139.9, 137.8, 126.9, 126.8, 124.9, 124.4, 81.6, 65.5, 48.2, 23.9; ν_{max} (KBr) 3011, 1771, 1478, 1322 cm^{-1}; HRMS (ESI): M^+, found 355.1208, $C_{23}H_{17}N_1O_3$ requires 355.1208.

FVP of **4c**. In a typical run, FVP of **4c** (30 mg, 0.085 mmol) at 360 °C produced a mixture, which was dissolved in chloroform (1–2 mL) and treated with anthracene (100 mg, 0.561 mmol) for 2 h at 60 °C. Reaction mixture was subjected to radial chromatography (petroleum ether–ethyl acetate 10:1, then the solvent polarity was gradually increased to 1:1) to obtain products, in order of elution: anthracene, **18**, and **17**.

*4.1.13. (2β,8β,10α,13α)-5,15-Di(p-methoxybenzyl)-5,15-diaza-17,18-dioxahexacyclo[7.4.3.^{10,13}.1^{2,8}.1^{10,13}.0^{1,9}.0^{3,7}]heptadeca-3,11-diene-4,6,14,16-tetraone (**17**).* Compound **17** (11 mg, 18%, mp 223–225 °C); δ_H (400 MHz, $CDCl_3$7.21 (2H, dd, J=3.5 , 5.2 Hz), 7.12 (2H, dd, J=3.2 , 5.5 Hz), 7.11 (2H, d, J=8.5 Hz), 6.98 (2H, dd, J=3.5 , 5.2 Hz), 6.77 (2H, d, J=8.5 Hz), 6.74 (2H, d, J=8.6 Hz), 6.70 (2H, d, J=8.6 Hz), 6.60 (2H, dd, J=3.2 , 5.5 Hz), 4.91 (2H, s), 5.87 (2H, s), 4.76 (2H, s), 4.66 (2H, s), 4.29 (2H, s), 3.99 (2H, s), 3.79 (3H, s),) 3.77 (3H, s); δ_C (100 MHz, $CDCl_3$) 175.6, 174.4, 159.3, 158.9, 140.8, 139.1, 138.8, 130.8, 130.4, 127.0, 126.9, 126.8, 126.6, 124.6, 124.1, 113.6, 113.4, 83.7, 78.2, 71.5, 63.6, 55.2, 50.9, 42.6, 42.0; ν_{max} (KBr) 2998, 1774, 1747, 1624, 1456 cm^{-1}; HRMS (ESI): M^+, found 718.2321, $C_{44}H_{34}N_2O_8$ requires 718.2315.

*4.1.14. (2α,9α,11α,14α)-16-Aza-18-oxaheptacyclo[8.4.3.4^{2,9}.1^{11,14}.0^{1,10}.0^{2,9}.0^{3,8}]tetracosa-3,5,7,12,19,21,23-heptaene-15,17-dione (**18**).* Compound **18** (3 mg, 10%, mp 178–181 °C); δ_H (400 MHz, $CDCl_3$) 7.20 (2H, dd, J=3.1 , 5.5 Hz), 6.84 (2H, d, J=8.6 Hz), 6.64 (2H, d, J=8.6 Hz); 6.69 (1H, s), 6.55 (2H, dd, J=3.1 , 5.5 Hz), 4.71 (2H, s), 5.81 (2H, s), 4.31 (2H, s); δ_C (100 MHz, $CDCl_3$) 175.5, 142.4, 139.2, 137.1, 126.8, 126.1, 124.5, 123.4, 81.7, 65.6, 24.9; ν_{max} (KBr) 3068, 2356, 1746, 1346 cm^{-1}; HRMS (ESI): M^+, found 341.1056, $C_{22}H_{15}N_1O_3$ requires 341.1052.

Monocrystals of **18** suitable for structural analysis were obtained by slow crystallization from CH_2Cl_2 solution. Crystal data: $C_{22}H_{15}N_1O_3$, M_r=341.35, Monoclinic, C2/*c*, *a*=27.608(2) Å, *b*=9.3019(8) Å, *c*=12.9135(11) Å, α=90°, β=98.499(2)°, γ=90°, *V*=3279.9(5) Å^3, *Z*=8, *T*=298(2) K, density=1.383 Mg/m^3, crystal size=0.21×0.17×0.11 mm^3. Final *R* indices [$I>2\sigma(I)$], *R*1=0.0614, wR2=0.1765. *R* indices (all data), *R*1=0.0723, *wR*2=0.1890. Data/restraints/parameters, 2882/0/235. Goodness-of fit on F^2, 1.054.

FVP of **4d**. In a typical run, FVP of **4d** (30 mg, 0.103 mmol) at 420 °C produced a mixture, which was dissolved in chloroform (1–2 mL) and treated with (100 mg, 0.561 mmol) for 2 h at 60 °C.

*4.1.15. (2α,9α,11α,14α)-16-Acethoxyaminoethyl-16-aza-18-oxa heptacyclo[8.4.3.4^{2,9}.1^{11,14}.0^{1,10}.0^{2,9}.0^{3,8}]tetracosa-3,5,7,12,19,21, 23-heptaene-15,17-dione (**19**).* (Estimated from crude reaction spectrum); δ_H (400 MHz, $CDCl_3$) 7.14 (4H, dd, J=3.2 , 5.4 Hz); 7.23–7.26 (4H, m), 6.38 (2H, s), 4.96 (2H, s), 4.73 (2H, s), 3.24 (2H, t, J=6.2 Hz), 3.13 (2H, t, J=6.2 Hz), 1.89 (3H, s).

*4.1.16. (2β,4α,11α,13β,15α,18α)-20,29-Di(acethoxyaminoethyl)-20,29-diaza-31,32-dioxaoctacyclo[12.4.3.6.^{4,11}.3^{3,12}.1^{2,13}.1^{15,18}.0^{1,14}.0^{3,12}.0^{5,10}.0^{22,27}]dotriaconta-5,7,9,16,22,24,26-heptaene-19,21,28,30-tetraone (**20**).* (Estimated from crude reaction spectrum); δ_H (400 MHz, $CDCl_3$) 7.16–7.25 (4H, m), 7.13 (2H, dd, J=3.2 , 5.4 Hz), 6.39 (2H, s), 4.94 (2H, s), 4.91 (2H, s), 4.65 (2H, s), 3.97 (2H,

t, J=5.3 Hz), 3.47 (2H, t, J=5.3 Hz), 3.32 (2H, t, J=5.6 Hz), 2.82 (2H, t, J=5.6 Hz), 1.96 (3H, s), 1.77 (3H, s).

*4.1.17. 1-Acethoxyaminoethyl-1-aza-5-oxabicyclo[3.3.0^{3,7}]octa-3,6-diene-2,8-dione (**6d**).* Compound **6d** (6 mg, 33%, mp 126–129 °C); δ_H (400 MHz, $CDCl_3$) 7.80 (2H, s), 4.29 (2H, t, J=5.6 Hz), 3.88 (2H, t, J=5.6 Hz), 2.00 (3H, s); δ_C (100 MHz, $CDCl_3$) 170.9, 161.5, 137.9, 122.2, 61.4, 37.6, 20.7; ν_{max} (KBr) 3156, 1810, 1775, 1397 cm^{-1}; HRMS (ESI): M$^+$, found 223.0483, $C_{10}H_9NO_5$ requires 223.0481.

FVP of **21**. In a typical run, FVP of **21** (20 mg, 0.081 mmol) at 340 °C produced a mixture, which was dissolved in chloroform (1–2 mL) and treated with anthracene (100 mg, 0.561 mmol) for 2 h at 60 °C. Reaction mixture was subjected to radial chromatography (petroleum ether–ethyl acetate 10:1, then the solvent polarity was gradually increased to 1:1) to obtain products, in order of elution **6b**, **23**, **24**.

*4.1.18. (2α,9α,11α,14α)-16-Methyl-16-aza-18-oxaheptacyclo[8.4.3.4^{2,9}.1^{11,14}.0^{1,10}.0^{2,9}.0^{3,8}]tetracosa-3,5,7,19, 21,23-hexaene-15,17-dione (**23**).* Compound **23** (10 mg, 35%, mp 226–227 °C); δ_H (400 MHz, $CDCl_3$) 0.89–0.99 (2H, m), 7.33 (2H, dd, J=3.3 , 5.3 Hz), 7.24 (2H, dd, J=3.3 , 5.3 Hz), 7.11 (2H, dd, J=3.3 , 5.3 Hz), 7.10 (2H, dd, J=3.3 , 5.3 Hz), 4.78 (2H, s), 4.46 (2H, dd, J=2.4 , 3.5 Hz), 2.45 (3H, s), 1.45–1.52 (2H, m); δ_C (100 MHz, $CDCl_3$) 176.9, 139.9, 139.8, 126.9, 126.7, 124.8, 124.4, 84.3, 79.9, 67.2, 48.6, 26.3; ν_{max} (KBr) 3121, 1734, 1428, 1287 cm^{-1}; HRMS (ESI): M$^+$, found 357.1357, $C_{23}H_{19}NO_3$ requires 357.1365.

*4.1.19. (2β,4α,11α,13β,15α,18α)-20,29-Dimethyl-20,29-diaza-31,32-dioxaoctacyclo[12.4.3.6.^{4,11}.3^{3,12}.1^{2,13}.1^{15,18}.0^{1,14}.0^{3,12}.0^{5,10} .0^{22,27}] dotriaconta-5,7,9,22,24,26-hexaene-19,21,28,30-tetraone (**24**).* Compound **24** (2 mg, 5%, mp 319–321 °C); δ_H (400 MHz, $CDCl_3$) 7.25 (2H, dd, J=3.3 , 5.5 Hz), 7.22 (2H, dd, J=3.3 , 5.5 Hz), 7.14 (2H, dd, J=3.1 , 5.3 Hz), 7.11 (2H, dd, J=3.1 , 5.3 Hz), 4.79 (2H, s), 4.68 (2H, s), 4.63 (2H, dd, J=1.1 , 5.2 Hz), 2.96 (3H, s), 2.05 (3H, s), 1.25–1.29 (2H, m), 0.84–0.90 (2H, m); δ_C (100 MHz, $CDCl_3$) 175.6, 175.5, 140.3, 135.2, 127.0, 126.7, 125.0, 124.2, 84.1, 75.1, 64.2, 32.2, 29.7, 27.1; ν_{max} (KBr) 3034, 1741, 1733, 1415, 1313 cm^{-1}; HRMS (ESI): M$^+$, found 508.1629, $C_{30}H_{24}N_2O_6$ requires 508.1634.

*4.1.20. 1-Methyl-1-aza-5-oxabicyclo[3.3.0^{3,7}]octa-3,6-diene-2,8-dione (**6b**).* Compound **6b** (2 mg, 16%, mp 112–113 °C); δ_H (400 MHz, $CDCl_3$) 3.47 (3H, s), 7.81 (2H, s); δ_C (400 MHz, $CDCl_3$) 66.2, 121.8, 138.1, 162.2; ν_{max} (KBr) 3047, 1768, 1389, 1209 cm^{-1}; HRMS (ESI): M$^+$, found 151.0271, $C_7H_5NO_3$ requires 151.0269.

*4.1.21. 4-Methyl-4-aza-10-oxatricyclo[5.2.1.0^{2,6}]deca-2-diene-3,5-dione (**22**).* (Estimated from crude reaction spectrum); δ_H (400 MHz, $CDCl_3$) 5.36 (2H, dd, J=1.6 , 3.1 Hz), 2.96 (3H, s), 1.37–1.42 (2H, m), 1.52–1.55 (2H, m); HRMS (ESI): M$^+$, found 179.0580, $C_9H_9N_1O_3$ requires 179.0582.

*4.1.22. (2β,8β,10α,13α)-5,15-Di(methyl)-5,15-diaza-17,18-dioxa hexacyclo[7.4.3.1^{2,8}.1^{10,13}.0^{1,9}.0^{3,7}]octadeca-3-ene-4,6,14,16-tetraone (**25**).* (Estimated from crude reaction spectrum); δ_H (400 MHz, $CDCl_3$) 5.59 (2H, s), 4.44 (2H, dd, J=2.2 , 3.5 Hz), 3.02 (3H, s), 3.00 (3H, s), 1.78–1.82 (2H, m), 1.08–1.12 (2H, m); HRMS (ESI): M$^+$, found 330.0850, $C_{16}H_{14}N_2O_6$ requires 330.0852.

4.2. Microwave-assisted reactions, general procedure

Imide substrates **4a**,**4b** (30 mg, 0.1 mmol), were subjected to MW irradiation at pre-set temperature for 5 min. After cooling, reaction mixture was dissolved in chloroform and treated with an excess of anthracene at 60 °C for 2 h. Obtained products were analysed by ^{1}H NMR spectroscopy.

4.3. Computational details

All geometrical optimizations were carried out employing B3LYP/6-31G*[17], BMK/6-31G* and M052X/6-31G* methods employing 6-31G* basis set. Calculations were performed using Gaussian03 suite of programs,[29] implemented on dual core Opteron 240 personal computer under Linux operating system and computer cluster Isabella at the Computing centre of the University of Zagreb. Activation energies were estimated, performing transition state (TS) calculations.[30] Harmonic vibration frequencies were calculated for all localized stationary structures to verify whether they are minima or transition states.

Acknowledgements

This research was funded by grants from the Australian Research Council (ARC) and the Croatian ministry of science, education and sport (No. 098-0982933-3218).

Supplementary data

Full crystallographic data for compound **18** have been deposited with the Cambridge Crystallographic Data Centre, deposition number CCDC 794352. These data can be obtained free of charge from The Cambridge Crystallographic Data Centre via www.ccdc.cam.ac.uk/data_request/cif. These data include MOL files and InChIKeys of the most important compounds described in this article.

References and notes

1. Margetić, D.; Warrener, R. N.; Butler, D. N. In *Paper no. 39, at the Sixth Electronic Computer Chemistry Conference (ECCC6)*; Homeier, H., Ed.; November 1–30, 1999; http://www.chemie.uni-regensburg.de/ECCC6/.
2. Brown, R. F. C. *Pyrolytic Methods in Organic Chemistry: Application of Flow and Flash Vacuum Pyrolytic Techniques*; Academic: New York, NY, 1980; McNab, H. *Aldrichimica Acta* **2004**, *37*, 19–26.
3. Butler, D. N.; Margetić, D.; O'Neill, P. J. C.; Warrener, R. N. *Synlett* **2000**, *1*, 98–100.
4. Margetić, D.; Warrener, R. N.; Sun, G.; Butler, D. N. *Tetrahedron* **2007**, *63*, 4338–4346.
5. Warrener, R. N.; Elsey, G. M.; Maksimović, L.; Johnston, M. R.; Kennard, C. H. L. *Tetrahedron Lett.* **1995**, *36*, 7753–7756.
6. We have observed a similar acetylene elimination from **2** at elevated temperatures (440 °C) gave novel 3,4-carboxylic furan anhydride **7**. However at the temperature required for furan elimination (370 °C), no **7** was produced.
7. Tietze, L. F.; Haunert, F. Domino Reactions in Organic Synthesis In *An Approach to Efficiency, Elegance, Ecological Benefit, Economic Advantage and Preservation of our Resources in Chemical Transformations. 'Stimulating Concepts in Chemistry'*; Shibasaki, M., Stoddart, J. F., Voegtle, F., Eds.; Wiley VCH: Weinheim, 2000; p 39.
8. Kaval, N.; Van der Eycken, J.; Caroen, J.; Dehaen, W.; Strohmeier, G. A.; Kappe, C. O.; Van der Eycke, E. *J. Comb. Chem.* **2003**, *5*, 560–568.
9. Head, N. J.; Oliver, A. M.; Look, K.; Lokan, N. R.; Jones, G. A.; Paddon-Row, M. N. *Angew. Chem., Int. Ed.* **1999**, *38*, 3219–3222.
10. Warrener, R. N.; Maksimović, L. *Tetrahedron Lett.* **1994**, *35*, 2389–2392.
11. Appukkuttan, P.; Mehta, V. P.; Van der Eycken, E. V. *Chem. Soc. Rev.* **2010**, *39*, 1467–1477.
12. Garrigues, P.; Garrigues, B. *C. R. Acad. Sci., Ser. IIC* **1998**, *1*, 545–550.
13. Cho, H. Y.; Ajaz, A.; Himali, D.; Waske, P. A.; Johnson, R. P. *J. Org. Chem.* **2009**, *74*, 4137–4142.
14. Boese, A. D.; Martin, J. M. L. *J. Chem. Phys.* **2004**, *121*, 3405–3416.
15. Zhao, Y.; Schultz, N. E.; Truhlar, D. G. *J. Chem. Theory Comput.* **2006**, *2*, 364–382.
16. *Modern Density Functional Theory: A Tool for Chemistry, Theoretical and Computational Chemistry*; Seminario, J. M., Politzer, P., Eds.; Elsevier: Amsterdam, 1995; Vol. 2.
17. Margetić, D.; Warrener, R. N. *Croat. Chem. Acta* **2003**, *76*, 357–363.
18. Margetić, D.; Warrener, R. N.; Malpass, J. R. *Internet J. Chem.* **1999**, *2* Article 6; http://www.ijc.com/.
19. Margetić, D.; Eckert-Maksić, M. *New J. Chem.* **2006**, *30*, 1149–1154.
20. Margetić, D.; Johnston, M. R.; Warrener, R. N. *Molecules* **2000**, *5*, 1417–1428.
21. Margetić, D.; Eckert-Maksić, M.; Trošelj, P.; Marinić, Ž *J. Flour. Chem.* **2010**, *131*, 408–416.
22. Margetić, D.; Trošselj, P.; Johnston, M.R. *Mini-Rev Org. Chem.*, in press; Margetić, D. *Trends Heterocycl. Chem.* **2009**, *14*, 79–89.
23. Borden, W. T. *Chem. Rev.* **1989**, *89*, 1095–1109.
24. Inagaki, H.; Fujimoto, H.; Fukui, K. *J. Am. Chem. Soc.* **1974**, *98*, 4054–4061.

25. Margetić, D.; Warrener, R. N.; Butler, D. N. In *Sixth Electronic Computational Chemistry Conference (ECCC-6), Paper 39*; Homeier, H. H., Ed.; November 1-30, 1999; http://www.chemie.uni-regensburg.de/ECCC6/.
26. Hehre, W. J. Chapter 27: Computational Chemistry In *Physical Chemistry*; Engel, T., Reid, P., Eds.; Prentice Hall: London, 2006; Hehre, W.J. Chapter 8.5. Spartan 5. 1 User's Guide, Wavefunction: Irvine, CA, 1997.
27. Liddell, M. J.; Margetić, D.; Mitchell, A. S.; Warrener, R. N. *J. Comput. Chem.* **2003**, *25*, 542–557.
28. Margetić, D. Ph.D. Thesis, Zagreb University, 1993; Warrener, R. N.; Wang, S.; Russell, R. A. *Tetrahedron* **1997**, *53*, 3975–3990.
29. Frisch, M. J.; Trucks, G. W.; Schlegel, H. B.; Scuseria, G. E.; Robb, M. A.; Cheeseman, J. R.; Montgomery, J. A., Jr.; Vreven, T.; Kudin, K. N.; Burant, J. C.; Millam, J. M.; Iyengar, S. S.; Tomasi, J.; Barone, V.; Mennucci, B.; Cossi, M.; Scalmani, G.; Rega, N.; Petersson, G. A.; Nakatsuji, H.; Hada, M.; Ehara, M.; Toyota, K.; Fukuda, R.; Hasegawa, J.; Ishida, M.; Nakajima, T.; Honda, Y.; Kitao, O.; Nakai, H.; Klene, M.; Li, X.; Knox, J. E.; Hratchian, H. P.; Cross, J. B.; Bakken, V.; Adamo, C.; Jaramillo, J.; Gomperts, R.; Stratmann, R. E.; Yazyev, O.; Austin, A. J.; Cammi, R.; Pomelli, C.; Ochterski, J. W.; Ayala, P. Y.; Morokuma, K.; Voth, G. A.; Salvador, P.; Dannenberg, J. J.; Zakrzewski, V. G.; Dapprich, S.; Daniels, A. D.; Strain, M. C.; Farkas, O.; Malick, D. K.; Rabuck, A. D.; Raghavachari, K.; Foresman, J. B.; Ortiz, J. V.; Cui, Q.; Baboul, A. G.; Clifford, S.; Cioslowski, J.; Stefanov, B. B.; Liu, G.; Liashenko, A.; Piskorz, P.; Komaromi, I.; Martin, R. L.; Fox, D. J.; Keith, T.; Al-Laham, M. A.; Peng, C. Y.; Nanayakkara, A.; Challacombe, M.; Gill, P. M. W.; Johnson, B.; Chen, W.; Wong, M. W.; Gonzalez, C.; Pople, J. A. *Gaussian 03, Revision B.03*; Gaussian: Wallingford, CT, 2003.
30. Houk, K. N.; Li, Y.; Evanseck, J. D. *Angew. Chem., Int. Ed.* **1992**, *31*, 682–708.